Bioprocess Biosyst Eng (2017) 40:943–957
DOI 10.1007/s00449-017-1758-2

RESEARCH PAPER

In vitro antioxidant and antidiabetic activities of zinc oxide nanoparticles synthesized using different plant extracts

Dilaveez Rehana[1,2] · D. Mahendiran[1] · R. Senthil Kumar[3] · A. Kalilur Rahiman[1]

Received: 16 November 2016 / Accepted: 7 March 2017 / Published online: 30 March 2017

Abstract Phytofabricated green synthesis of zinc oxide (ZnO) nanoparticles using different plant extracts of *Azadirachta indica, Hibiscus rosa-sinensis, Murraya koenigii, Moringa oleifera*, and *Tamarindus indica* for biological applications has been reported. ZnO nanoparticles were also synthesized by chemical method to compare the efficiency of the green synthesized nanoparticles. FT-IR spectra confirmed the functional groups involved in the green synthesis of ZnO nanoparticles and the powder XRD patterns of the ZnO nanoparticles revealed pure wurtzite structure with preferred orientation at (100) reflection plane. SEM and TEM analysis revealed the spherical shape of the synthesized ZnO nanoparticles with the particle size between 54 and 27 nm. The antioxidant activity was evaluated by five different free radical scavenging assays. The present study also intends to screen α-amylase and α-glucosidase activity of ZnO nanoparticles synthesized using natural sources, which may minimize the toxicity and side effects of the inhibitors used to control diabetes. The ZnO nanoparticles synthesized using *T. indica* extract displayed remarkable antioxidant and antidiabetic activities.

Keywords Green synthesis · Zinc oxide nanoparticles · Phytochemical studies · Antioxidant activity · Antidiabetic activity

✉ A. Kalilur Rahiman
akrahmanjkr@gmail.com; akrahmanjkr@thenewcollege.in

[1] Department of Chemistry, The New College (Autonomous), Chennai 600 014, India

[2] Department of Chemistry, Justice Basheer Ahmed Sayeed College for Women (Autonomous), Chennai 600 018, India

[3] Department of Pharmaceutical Chemistry, Swamy Vivekanandha College of Pharmacy, Tiruchengodu 637 205, India

Introduction

Nanomaterials, due to their large surface area and wider bandgap between valence and conduction band, show atom like behavior when divided to near atomic size, which results from higher surface energy [1]. The worldwide nanotechnology revolution is predicted to impact several areas of biomedical research such as drug delivery, cell imaging, and cancer therapy [2]. Nanomaterials can kill some 650 cells, while the antibiotics kill half dozen different disease causing organisms, and hence are called wonder of modern medicine [3]. A number of metal oxide nanoparticles have been reported, but zinc oxide is a unique and key material that possesses characteristic features such as crystal size, orientation and morphology aspect ratio, and crystalline density with direct bandgap of 3.3 eV at room temperature and high exciton binding energy of 60 meV, and finds applications in wide area of science and technology [4–6]. Nano ZnO can absorb both UV-A and UV-B radiations, while TiO_2 can only block UV-B and there by offering better protection and improved opaqueness, and hence may overtake nano TiO_2 in near future [7].

The synthesis of nanoparticles using chemical methods leads to some toxic chemicals adsorbed on the surface that may have adverse effects on medicinal applications. The development of an eco-friendly and compatibility approach for the synthesis of nanoparticles has created an increasing awareness towards green chemistry due to the use of environmentally benign materials like plant extracts, bacteria, fungi, and enzymes [1, 8]. Plants are a rich source of

secondary metabolites and novel therapeutic compounds, which enhance human health with controlled adverse effect. The importance of plant mediated biological synthesis of nanoparticles is due to its simplicity, ecofriendliness, and extensive biological activity [9, 10]. Plants such as *Citrus limon, Ocimum sanctum*, and *Lemon grass* have been used to synthesize Ag and Au nanoparticles, and *Aloe vera* leaf extract in the synthesis of ZnO nanoparticles was also reported [11, 12]. Alkaloids, flavonoids, saponins, steroids, terpenoids, polysaccharides, and tannins are important bioactive clusters in plants, which largely contribute to various technological activities in the traditional and therapeutic principles [13].

The pharmacological activities of the medicinally important plants have been reported. *Azadirachta indica* is a tropical ever green native tree to India, and known as 'the village pharmacy' because of its healing versatility and medicinal properties. The *A. indica* leaf extract acts as an antihyperglycemic agent in IDDM (Insulin Dependent Diabetes Mellitus) and NIDDM (Non-Insulin-Dependent Diabetes Mellitus) [14]. *Hibiscus rosa-sinensis* is widely cultivated in the tropics as an ornamental plant, belongs to Malvaceae family, and exhibits spermatogenic, antidiabetic, and antioxidant activities [15, 16]. The plant *Murraya koenigii* is native to india and belongs to the family Rutaceae, and has strong antioxidative activities due to the presence of carbazole [17]. Hence, different parts of *M. koenigii* plant are used in medicine as a tonic for stomach ache, as stimulant and carminative [18, 19], hypoglycemic agent [20] antifungal agent [21], and also exhibit cytotoxicity against colon cancer [22]. *Moringa oleifera* is fast-growing ornamental tree which belongs to the single genus of family Moringaceae and was extensively used as immune boosting agent and regulator for blood sugar and cholesterol and in the treatment of inflammation, cardiovascular, and liver diseases [23, 24]. *Tamarindus indica* is one of the most important plant resources as food materials, which is used to prepare beverages and to flavor confections, curries and sauces, and it is accepted as herbal medicine in parts of the world [25]. *T. indica* was found to have potent antidiabetic and antihyperlipidemic activities that reduce blood sugar level, total cholesterol and triglycerides, respectively, in streptozotocin (STZ)-induced diabetic male rat [26].

ZnO nanoparticles has drawn much attention towards biological applications such as biological sensing, biological labeling, gene delivery, drug delivery, and nanomedicine, which also exhibit antibacterial, antifungal, acaricidal, pediculocidal, larvaecidal, and antidiabetic activities. To the best of our knowledge, there are scarce reports pertaining to the in vitro antioxidant and antidiabetic properties of the ZnO nanoparticles synthesized using plant extracts [27], which encouraged us to synthesis ZnO nanoparticles using the plant extracts of *A. indica, H. rosa-sinensis, M. koenigii, M. oleifera*, and *T. indica*, and investigate their antioxidant and antidiabetic activities.

Experimental

Materials and plant extracts preparation

Zinc nitrate hexahydrate and sodium hydroxide were procured from Sigma–Aldrich, India. Fresh leaves of *A. indica, H. rosa-sinensis, M. koenigii, M. oleifera*, and *T. indica* free from disease were collected and authenticated by Plant Research Centre, Chennai. The collected leaves were washed thoroughly 2–3 times with running tap water followed by double-distilled water. Then, the leaves were dried at room temperature and 20 g of leaves were boiled with 100 mL of double-distilled water for 20 min at 60 °C during which a light yellow colored solution was formed. The solution was cooled to room temperature, and filtered with Whatman No.1 filter paper and stored in the refrigerator until further use. ZnO nanoparticles were successfully synthesized using these plant extracts and chemical method by adopting the reported procedure [28, 29].

Synthesis of zinc oxide nanoparticles

Synthesis of zinc oxide nanoparticles by chemical method

Zinc nitrate hexahydrate (0.2 mol) and equimolar amount of NaOH were dissolved in deionized water and stirred at 80 °C until a homogeneous solution was formed. It was allowed to maintain at room temperature for 1 h to form a white precipitate, centrifuged, washed several times with deionized water followed by ethanol, and dried in a hot air oven for 2 h at 120 °C.

Green synthesis of zinc oxide nanoparticles using different leaf extracts

Zinc nitrate hexahydrate (2 g) in aqueous plant extract (20 mL) was dissolved under constant stirring using magnetic stirrer. After complete dissolution of the mixture, the solution was boiled at 70 °C with continuos stirring until the formation of deep yellow colored paste. The paste was then transferred to a ceramic crucible and heated in furnace at 400 °C for 2 h, resulting in pale white colored powder.

The chemically synthesized ZnO nanoparticles were designated as ZnO-S1, while that synthesized by green method using various plant extracts such as *A. indica, H. rosa-sinensis, M. koenigii, M. oleifera*, and *T. indica* were designated as ZnO-S2, ZnO-S3, ZnO-S4, ZnO-S5, and ZnO-S6, respectively.

Characterization

FT-IR spectra of the synthesized ZnO nanoparticles were recorded at room temperature on Shimadzu IR460 spectrophotometer in the range 4000–400 cm^{-1}. X-ray diffraction patterns were recorded using Siefert Analyze diffractometer with Cu Kα radiation (λ = 0.15406 Å) and the maximum peak position was compared with the standard files to identify the crystalline phase. UV–Vis spectra were recorded using UV140404B in the wavelength range 200–900 nm in reflectance mode. Photoluminescence spectra were recorded using FLUOROLOG-FL3-11fluorescence spectrometer. The morphology was studied using SEM (Hitachi SU6600) and TEM (TEM CM 200). The energy dispersive X-ray spectroscopy (EDX, BURKER, INDIA) analyses were carried out to confirm the chemical composition of zinc and oxygen elements.

Phytochemical studies

The leaf extracts of *A. indica, H. rosa-sinensis, M. koenigii, M. oleifera*, and *T. indica* were subjected to phytochemical tests for the identification of their active constituents [30–32].

Detection of alkaloids

To 3 mL of the extract, 0.20 mL of dilute hydrochloric acid was added and divided into four parts, and each part was treated with Mayer's reagent, Dragendroff's reagent, Hager's reagent, and Wagner's reagent. All the tests gave negative results, indicating the absence of alkaloids in the extracts.

Detection of carbohydrates and glycosides

To 3 mL of plants extracts, 4 mL of distilled water was added, and divided into two parts. To one part of the extract, 0.15 mL of 1% alcoholic α-naphthol and 2 mL of concentrated sulphuric acid were added along the sides of the test tube. The appearance of brown ring at the junction of two liquids shows the presence of carbohydrates. To another portion of the extract, 1 mL of Fehling's solution A and B was added and heated on a water bath. The formation reddish colored precipitate shows the presence of carbohydrates.

To detect the presence of glycosides, the plant extracts (3 mL) were hydrolyzed with dilute hydrochloric acid for 1–2 h on a water bath and the hydrolysate was divided into two portions. To one portion of the hydrolysate, 1 mL of pyridine and 0.20 mL of sodium nitroprusside solution were added and made alkaline with 0.60 mL sodium hydroxide solution, which turns into red colored solution. Another portion of hydrolysate was treated with chloroform (1 mL) and the chloroform layer was separated, and dilute ammonia solution (1 mL) was added, which turns into pink colored solution. This test shows the presence of glycosides.

Detection of fixed oils and fat

About 3 mL of plant extracts were pressed between two filter papers. The absence of oil stain on the papers indicates the absence of fixed oil. To 3 mL of extract, 0.20 mL of 0.5 N alcoholic potassium hydroxide was added along with a 0.05 mL of phenolphthalein and the mixture was heated on a water bath for 1–2 h during which no soap formation was observed, indicating the absence of fixed oils and fats.

Detection of flavonoids

The plant extracts (3 mL) with aqueous sodium hydroxide (0.20 mL) produced yellow colour, while with concentrated sulphuric acid (0.20 mL) produced yellow orange colour. The extracts also show positive result in Shinoda's test in which the extract in alcohol and a piece of magnesium in the presence of conc. hydrochloric acid produced magenta colour on heating. These results show the presence of flavonoids in the extracts.

Detection of phytosterols

To 3 mL of plant extracts, 5 mL of chloroform was added. No colour change was observed when these chloroform solution was treated with concentrated sulphuric acid (0.20 mL) or with concentrated sulphuric acid (0.20 mL) followed by dilute acetic acid (0.20 mL) and acetic anhydride (3 mL), which indicates the absence of phytosterols in the extracts.

Detection of proteins and free amino acids

To 3 mL of plant extracts, equal volume of 5% sodium hydroxide and 1% copper sulphate solution was added. Violet colour was observed only for the extracts of *M. oleifera* and *T. indica*. These extracts also reacted with ninhydrin reagent, which gave purple colour. The obtained result indicates the presence of proteins and free amino acids in these extracts.

Detection of saponins

To 3 mL of plant extracts, 20 mL of distilled water was added and agitated in a measuring cylinder for 15 min. The formation of 1 cm layer of foam shows the presence of saponins in the extracts.

Detection of tannins and phenolic compounds

All the extracts (3 mL), with 5% ferric chloride solution produced violet colour, with 1% solution of gelatin containing 10% sodium chloride produced white precipitate, and with 10% lead acetate solution produced white precipitate. These results indicate the presence of tannins and phenolic compounds in the extracts.

In vitro antioxidant activity

Antioxidants are used in the treatment of various diseases and hence the antioxidant potential of the synthesized ZnO nanoparticles was studied using standard in vitro methods. These methods are based on inhibition of free radical measurements, which vary greatly according to the generation of radical, its reproducibility, and the end point. The concentrations of the ZnO nanoparticles and standard solutions used were 100, 50, 25, 12.5, 6.25, 3.12, and 1.56 µg/mL. The suspensions of ZnO nanoparticles were sonicated using a sonicator bath at room temperature for 30 min to avoid nanoparticles agglomeration. The samples were added to free radical-generating system, and the inhibition of the free radical action is measured and related to antioxidant activity. The absorbance was measured spectrophotometrically against the corresponding blank solutions and the percentage inhibition was calculated using the following formula:

$$\text{Radical scavenging activity (\%)} = \frac{\text{OD}_{\text{control}} - \text{OD}_{\text{sample}}}{\text{OD}_{\text{control}}} \times 100.$$

ABTS assay

2,2′-Azino-bis(3-ethylbenzothiazoline-6-sulphonic acid) diammonium salt (ABTS, 54.8 mg, 2 mM) was dissolved in distilled water (50 mL) followed by potassium persulphate (0.3 mL, 17 mM). The reaction mixture was kept at room temperature overnight in dark before usage. To 0.2 mL of various concentrations of the sample, 1.0 mL of freshly distilled DMSO and 0.16 mL of ABTS solution were added to make a final volume of 1.36 mL. After 20 min, absorbance was measured spectrophotometrically at 734 nm [33].

DPPH assay

The assay was carried out in a 96 well microtitre plate. To 200 µL of 2,2′-diphenyl-1-picrylhydrazyl (DPPH) solution, 10 µL of each of the sample or standard solution was added separately in wells of the microtitre plate. The plates were incubated at 37 °C for 30 min and the absorbance of each solution was measured at 490 nm [34].

Hydroxyl radical scavenging assay (p-NDA method)

To a reaction mixture containing ferric chloride (0.5 mL, 0.1 mM), EDTA (0.5 mL, 0.1 mM), ascorbic acid (0.5 mL, 0.1 mM), hydrogen peroxide (0.5 mL, 2 mM), and *p*-nitroso dimethylaniline (*p*-NDA, 0.5 mL, 0.01 mM) in phosphate buffer (pH 7.4, 20 mM), various concentrations of sample or standard (0.5 mL) were added to make a final volume of 3 mL. Sample blank was prepared by adding 0.5 mL sample and 2.5 mL of phosphate buffer. Absorbances of these solutions were measured at 440 nm [35].

Superoxide radical scavenging assay

To 1 mL of alkaline dimethyl sulfoxide (1 mL DMSO containing 5 mM NaOH in 0.1 mL water) and 0.3 mL of the sample in freshly distilled DMSO at various concentrations, 0.1 mL of nitroblue tetrazolium (NBT, 1 mg/mL) was added to make a final volume of 1.4 mL. The absorbance was measured at 560 nm [36].

Hydrogen peroxide radical scavenging assay

In this method, the decay or loss of hydrogen peroxide is measured spectrophotometrically [36]. A solution of hydrogen peroxide (20 mM) was prepared in phosphate buffered saline (PBS, pH 7.4). Various concentrations of 1 mL of the sample or standard in methanol were added to 2 mL of hydrogen peroxide solution in PBS. After 10 min, the absorbance was measured at 230 nm.

In vitro antidiabetic activity

α-Amylase inhibitory activity

α-Amylase (0.05 g of α-amylase in 100 mL of ice-cold distilled water) was pre-mixed with the synthesized ZnO nanoparticles at different concentrations (100–1.52 µg/mL) and sonicated at room temperature for 30 min to avoid nanoparticles agglomeration. Starch as a substrate was added as a 0.5% starch solution in phosphate buffer to start the reaction. The reaction was carried out for 20 min and terminated by adding 2 mL of DNS reagent (1% 3,5-dinitrosaliycilic acid and 12% sodium potassium tartrate in 0.4 M NaOH). The reaction mixture was then heated for 15 min at 100 °C and α–amylase activity was determined by measuring the absorbance at 540 nm [37]. Inhibition rates were calculated as percentage controls using the following formula:

$$I_{\alpha-\text{Amylase}}(\%) = \frac{A_{420\ \text{control}} - A_{420\ \text{sample}}}{A_{420\ \text{control}}} \times 100.$$

α-Glucosidase inhibitory activity

α-Glucosidase (0.05 g of α-glucosidase in 100 mL of ice-cold distilled water) was pre-mixed with the synthesized ZnO nanoparticles at various concentrations (100–1.52 µg/mL) and sonicated at room temperature for 30 min to avoid nanoparticles agglomeration. To start the reaction, *p*-nitrophenyl-α-D-glucopyranoside (3 mM) as a substrate in potassium phosphate buffer was added to the mixture. The reaction was incubated at 37 °C for 30 min and terminated by addition of Na_2CO_3 (2 mL, 0.1 M). α-Glucosidase activity was determined by measuring the release of *p*-nitrophenyl-α-D-glucopyranoside at 420 nm [38]. Inhibition rates were calculated as percentage controls using the following formula:

$$I_{\alpha-\text{Glucosidase}}(\%) = \frac{A_{420\ \text{control}} - A_{420\ \text{sample}}}{A_{420\ \text{control}}} \times 100.$$

Results and discussion

An eco-friendly method has been followed to synthesize ZnO nanoparticles using different leaf extracts of medicinally significant plants such as *A. indica, H. rosa-sinensis, M. koenigi, M. oleifera*, and *T. indica* (Fig. 1). ZnO nanoparticles were also synthesized by chemical method for comparison purpose. Preliminary phytochemicals screening showed the presence of phenolic and flavonoid compounds in the extracts. The presence of phenolic compounds in all the extracts encouraged us to evaluate the antioxidant activity of the synthesized ZnO nanoparticles. All the plants have good therapeutic potential, and hence antidiabetic activity was also investigated.

Identification of secondary metabolites in plant extracts

Preliminary phytochemical analysis was carried out for all the plant extracts, which shows positive result of carbohydrates, flavonoids, glycosides, phenolic compounds, proteins and amino acids, saponins, and tannins (Table 1). The bioactivities of these medicinal plants can be attributed to the presence of these phytochemical compounds [39].

Characterization of ZnO nanoparticles

FT-IR analysis

FT-IR spectra confirm the formation of ZnO nanoparticles synthesized using chemical and green methods (Fig. 2). All the samples exhibits a band at 454–481 cm^{-1} attributed to the bending vibration of Zn–O. The broad band in the region 3413–3475 cm^{-1} can be assigned to O–H stretching vibration, and the strong band observed at 1509–1577 cm^{-1} is assigned to the vibrations of H–O–H bond. The weak absorption band observed for the green synthesized ZnO nanoparticles in the region 2920–2936 cm^{-1} corresponds to C–H stretching in alkanes, and the strong band observed at 1414–1454 cm^{-1} is assigned to C–C stretching of the aromatic group [29]. The medium absorption band observed

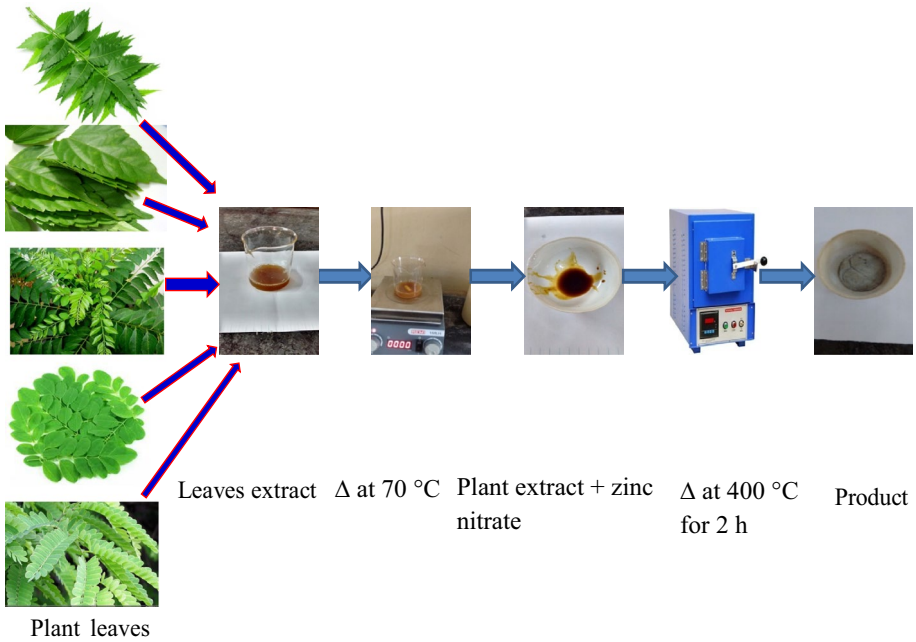

Fig. 1 Flow chart for the synthesis of ZnO nanoparticles using various plant extracts

Table 1 Phytochemical screening of the aqueous leaf extracts

Secondary metabolites	*Azadirachta indica*	*Hibiscus rosa-sinensis*	*Murraya koenigii*	*Moringa oleifera*	*Tamarindus indica*
Alkaloids	−	−	−	−	−
Carbohydrates	+	+	+	+	+
Flavonoids	+	+	+	+	+
Glycosides	+	+	+	+	+
Phenolic compounds	+	+	+	+	+
Phytosterols	−	−	−	−	−
Proteins and amino acids	−	−	−	+	+
Saponins	+	+	+	+	+
Tannins	+	+	+	+	+
Volatile oils	−	−	−	−	−

+ present, − absent

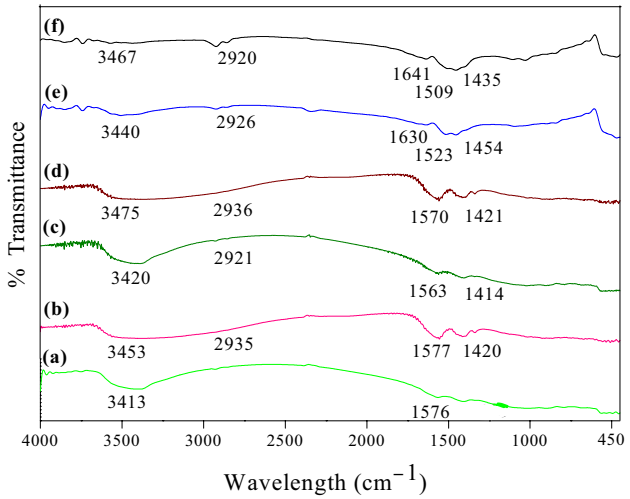

Fig. 2 FT-IR spectra of ZnO nanoparticles synthesized using chemical method; ZnO-S1 (*a*), and plant extracts; ZnO-S2 (*b*), ZnO-S3 (*c*), ZnO-S4 (*d*), ZnO-S5 (*e*), and ZnO-S6 (*f*)

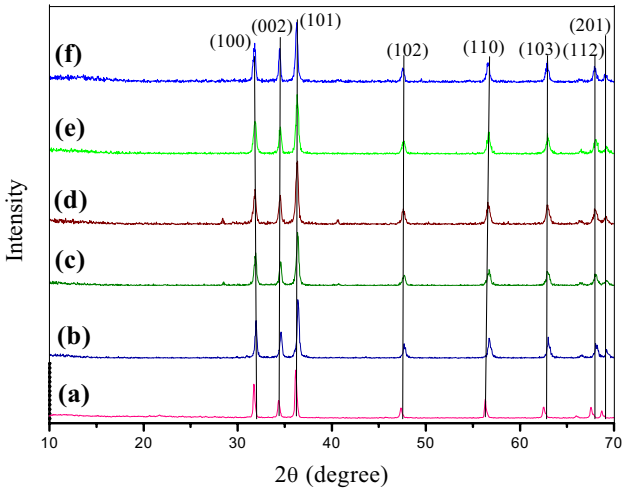

Fig. 3 XRD patterns of ZnO nanoparticles synthesized using chemical method; ZnO-S1 (*a*), and plant extracts; ZnO-S2 (*b*), ZnO-S3 (*c*), ZnO-S4 (*d*), ZnO-S5 (*e*), and ZnO-S6 (*f*)

at 1630 and 1641 cm^{-1} for the samples ZnO-S5 and ZnO-S6, respectively, corresponds to N–H vibration of primary amines. The obtained results suggest that the biological molecules were bound to the surface of the ZnO nanoparticles synthesized by green method, which could perform dual function of formation and stabilization of ZnO nanoparticles in the aqueous medium.

XRD analysis

XRD patterns of ZnO nanoparticles synthesized using chemical and green methods are shown in Fig. 3. ZnO nanoparticles synthesized by chemical method exhibited diffraction peaks at 2θ values 31.95°, 34.60°, 36.42°, 47.68°, 56.73°, 63.00°, 67.88°, and 69.32° corresponding to the plane of reflections (100), (002), (101), (102), (110), (103), (112), and (201), respectively, and in good agreement with joint committee on powder diffraction standards (JCPDS) card No: 036-1451. The XRD patterns of all the other ZnO nanoparticles synthesized using green method show similar diffraction peaks without considerable shift in the peak positions. All the peaks due to ZnO nanoparticles are well matched with the standard diffraction pattern of hexagonal crystal structure. The sharp and well-defined peaks indicate the crystalline nature of the synthesized ZnO nanoparticles (Table 2). The mean crystalline size of the nanoparticles was determined using the Scherrer's equation [40]:

$$D = 0.9\lambda/(\beta \cos\theta)$$

Table 2 Average crystallite size, lattice parameters, and band-gap values of ZnO nanoparticles determined by XRD, TEM, and DRS-UV techniques

Samples	Average crystallite size (nm) (XRD)	Lattice parameter (Å) (XRD)		Particle size (nm) (TEM)	Bandgap (eV) (DRS-UV)
		a-Axis	*c*-Axis		
ZnO-S1	54.58	3.250	5.2070	54.55	3.16
ZnO-S2	32. 69	3.246	5.2054	32.11	3.18
ZnO-S3	30.38	3.250	5.2070	30.33	3.20
ZnO-S4	30.39	3.242	5.2050	30.50	3.19
ZnO-S5	27.61	3.248	5.2062	27.45	3.21
ZnO-S6	25.66	3.250	5.2050	25.20	3.22

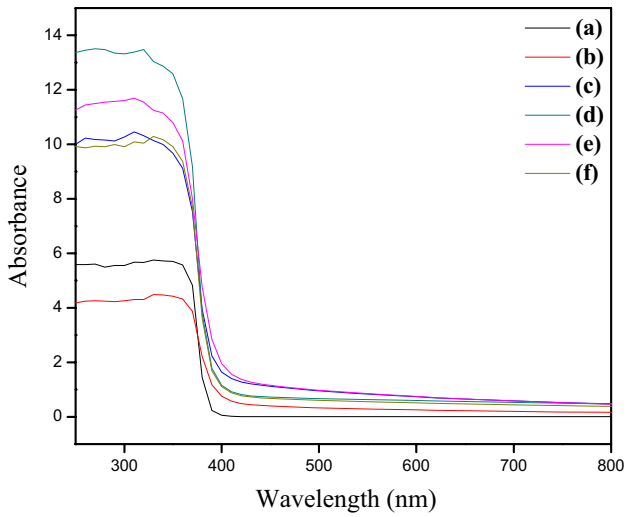

Fig. 4 UV–Vis spectra of ZnO nanoparticles synthesized using chemical method; ZnO-S1 (*a*), and plant extracts; ZnO-S2 (*b*), ZnO-S3 (*c*), ZnO-S4 (*d*), ZnO-S5 (*e*), and ZnO-S6 (*f*)

where λ is the wavelength, β is the full line width at half-maximum (FWHM) of the main intensity peak, and θ is the diffraction angle.

Optical properties of ZnO nanoparticles

UV–Vis spectra of ZnO nanoparticles synthesized by chemical and green methods are shown in Fig. 4. The characteristic absorption band at 385 nm is attributed to the intrinsic band-gap absorption of ZnO nanoparticles owing to the electron transition from the valence band to the conduction band ($O_{2p} \rightarrow Zn_{3d}$) [41]. The reflectance spectra were analyzed using the Kubelka–Munk relation. To convert Kubelka–Munk function, the following relation was used:

$$F(R) = (1-R)^2/2R$$

where R is the reflectance value. Band-gap energy of the samples was estimated from the variation of the Kubelka–Munk function with photon energy (Fig. 5). The band-gap value of ZnO nanoparticles is found to be in the range between 3.16 and 3.22 eV [3].

The PL emission spectra of ZnO nanoparticles synthesized using chemical and green methods are shown in Fig. 6. All the particles exhibited excitation and emission at different wavelength. The emission observed at 400–430 nm corresponds to the violet emission [42]. The green band in the range 550–600 nm and the red band in the range 600–675 nm may be correlated to a transition between the oxygen vacancy and interstitial oxygen [43, 44].

SEM, TEM, and EDX analysis

SEM and TEM images of ZnO nanoparticles synthesized using chemical and green methods are shown in Figs. 7 and 8. SEM images revealed the agglomeration of nanoparticles, and the individual nanoparticles are more or less spherical and granular in shape. TEM images shows spherical and hexagonal phase, which are in accordance with XRD data. The particle size for ZnO nanoparticles synthesized using plant extracts is in the range between 25 and 32 nm and are in accordance with that determined by XRD. TEM measurements are based on the visible grain boundaries, while the XRD calculation measures the extended crystalline region that diffracts X-ray coherently [45]. Small particles have larger surface area-to-volume ratio and represent a higher energy state than large particles. The SAED (selected area electron diffraction) pattern indicates highly polycrystalline structure of ZnO nanoparticles (Fig. 8f). The EDX analysis confirmed the chemical composition of ZnO nanoparticles (Fig. 9). The strong peaks are observed due to Zn and O atom, while the weak peaks are due to S, K, Cl, P, and Ca, which arises from the X-ray emission of macromolecules such as alcohols or phenolic compounds [46].

Free radical scavenging activity of ZnO nanoparticles

Even though in vitro methods provide a useful indication of antioxidant activities, results obtained from in vitro methods are difficult to apply to biological systems and do not inevitably predict a similar in vivo antioxidant activity. A number of different methods may be necessary to adequately assess in vitro antioxidant activity of a specific compound. All the methods that are developed have strengths and limitations and a single measurement of antioxidant capacity usually is not sufficient. In vitro

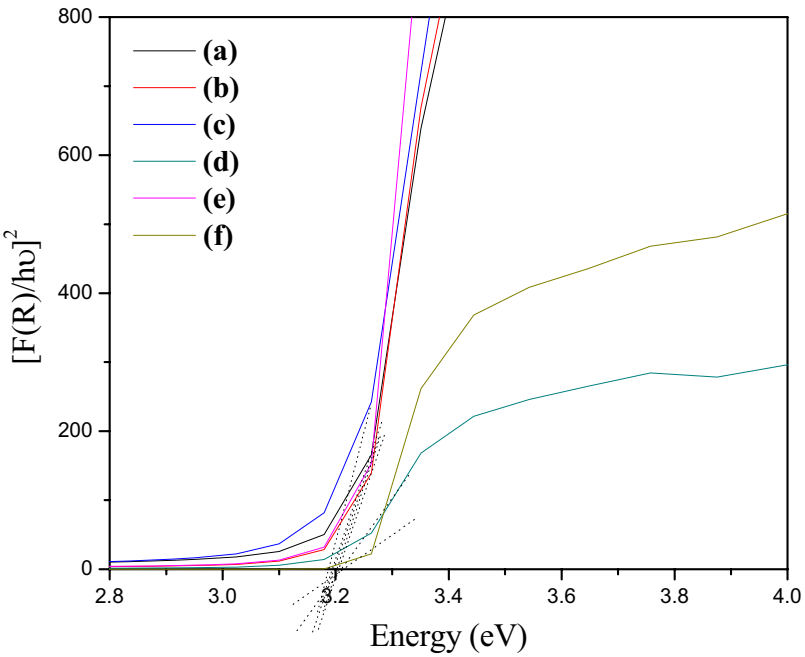

Fig. 5 Plots of estimated bandgap of ZnO nanoparticles synthesized using chemical method; ZnO-S1 (*a*), and plant extracts; ZnO-S2 (*b*), ZnO-S3 (*c*), ZnO-S4 (*d*), ZnO-S5 (*e*), and ZnO-S6 (*f*)

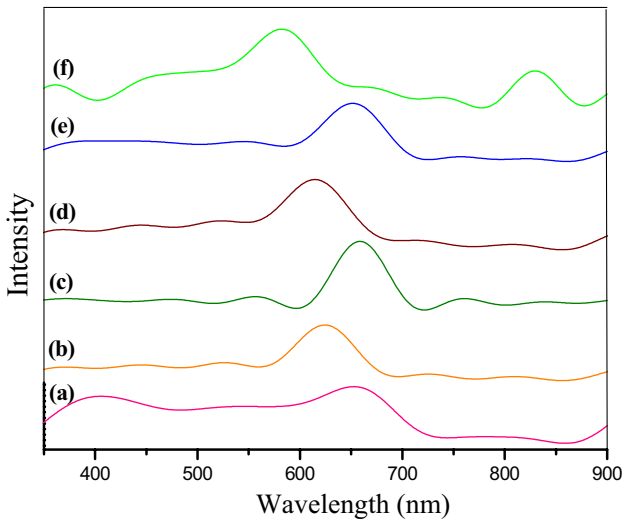

Fig. 6 Photoluminescence spectra of ZnO nanoparticles synthesized using chemical method; ZnO-S1 (*a*), and plant extracts; ZnO-S2 (*b*), ZnO-S3 (*c*), ZnO-S4 (*d*), ZnO-S5 (*e*), and ZnO-S6 (*f*)

antioxidant activity of the synthesized ZnO nanoparticles was investigated using ABTS, DPPH, superoxide, hydrogen peroxide, and hydroxyl radical scavenging assays with respect to the standard antioxidants ascorbic acid and rutin (Table 3).

ZnO nanoparticles synthesized by chemical method did not show antioxidant activity in any of the in vitro assays. However, the ZnO nanoparticles synthesized using plant extracts exhibit appreciable radical scavenging activity. Phytochemical analysis indicates that all the extracts derived from five different plants (*A. indica, H. rosa-sinensis M. koenigi, M. oleifera*, and *T. indica*) are rich in carbohydrates, flavonoids, glycosides, phenolic compounds, saponins, and tannins. The plant extracts enriched with these natural compounds are very well known for their antioxidant activity, and the zinc oxide nanoparticles synthesized using these plants extracts exhibit enhanced antioxidant activity. The mechanisms of action of flavonoids are through free radical scavenging or chelating process. Flavonoids have also been shown to treat many human diseases such as diabetes, cancer, and coronary heart disease, and also exhibit the antioxidative, antiviral, antimicrobial, and antiplatelet activities [27]. Phenolic compounds possess hydroxyl and carboxyl groups, which are able to bind to metals [47]. Based on the obtained antioxidant results, all the ZnO nanoparticles synthesized using plant extracts showed significant antioxidant activity with respect to standard antioxidants ascorbic acid and rutin. The observed order of antioxidant activity is as follows: ZnO-S6 > ZnO-S5 > ZnO-S3 > ZnO-S4 > ZnO-S2 > ZnO-S1. An important feature of ZnO nanoparticles is their ability to induce reactive oxygen species (ROS) generation, which can lead to cell death with increased antioxidant activity [48]. Antioxidants play an important role in the functioning of all biosystems where free radicals are generated due to interaction of biomolecules with molecular oxygen resulting in the degradation of biomolecules. They play a crucial role in scavenging these toxic free radicals thereby terminating the oxidative damage of human body [49]. Synthesis of ZnO nanoparticles is of great interest, because there are some factors believed to cause properties of nanomaterials

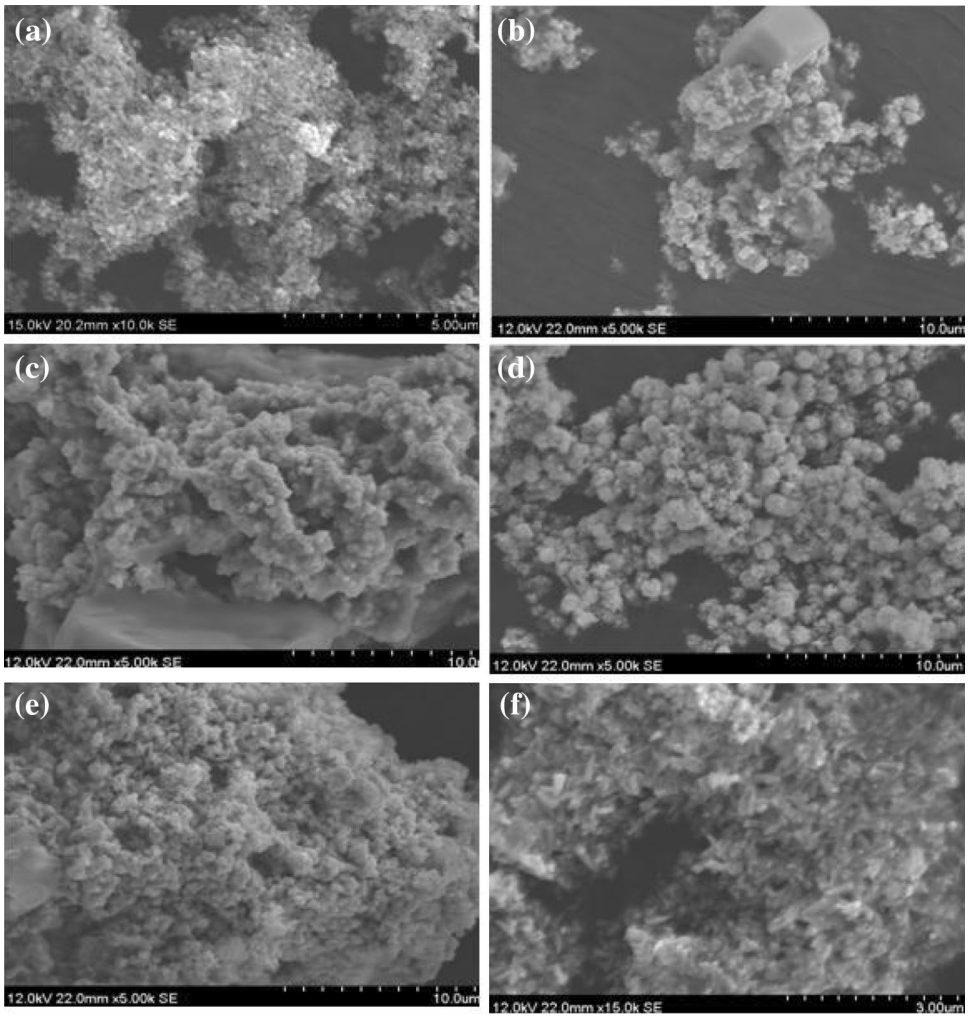

Fig. 7 SEM images of ZnO nanoparticles synthesized using chemical method; ZnO-S1 (**a**), and plant extracts; ZnO-S2 (**b**), ZnO-S3 (**c**), ZnO-S4 (**d**), ZnO-S5 (**e**), and ZnO-S6 (**f**)

to differ from their bulk counterparts including size of the nanoparticles, an increase in relative surface area, a greater percentage of atoms at the material's surface, and quantum effects [50]. The decrease in size results in increased interstitial zinc ions and oxygen vacancies improving the efficiency of the nanoparticles and also causes an increase in the bandgap [51, 52]. Small size of the nanoparticles allows their internalization into cells, and to interact with biomolecules within or on the cell surface, enabling them potentially to affect cellular responses in a dynamic and selective manner that makes them well suited for biological applications [53].

ABTS radical scavenging activity is often used for screening of complex antioxidant mixtures due to the involvement of drastic free radical, which are chemically produced. The solubility in both the organic and aqueous media and the stability in a wide pH range raised the interest in the use of $ABTS^{\cdot+}$ for the estimation of the antioxidant activity [27]. DPPH is a stable compound and accepts hydrogen or electrons [54]. The effect of antioxidants on DPPH radical scavenging is thought to be due to their hydrogen donating ability to become a stable diamagnetic molecule. Superoxide is oxygen centered radical with selective reactivity exhibiting limited chemical reactivity due to the generation of more dangerous species including singlet oxygen and hydroxy radicals, which causes the peroxidation of lipids. Superoxide can reduce certain iron complexes such as cytochrome. Superoxide anions are thus precursors to active free radical that have potential for reactivity with biological molecules and there by inducing tissues damage [55]. Hydrogen peroxide assay give rise to hydroxyl radicals in cells, which itself is not very reactive but sometimes toxic to the cells [56]. Lipid oxidation and enormous biological damage are caused due to hydroxy radicals, which are the major active oxygen species [57]. The ZnO-S6 nanoparticles exhibited potent hydrogen peroxide scavenging activity by inhibition of bleaching of *p*-NDA with respect to the standards. In this reaction, iron-EDTA complex reacts with hydrogen peroxide in the presence of antioxidant to generate hydroxyl radical, which can bleach *p*-NDA specifically. The ZnO nanoparticles synthesized using the extracts of *M. oleifera* and *T. indica*

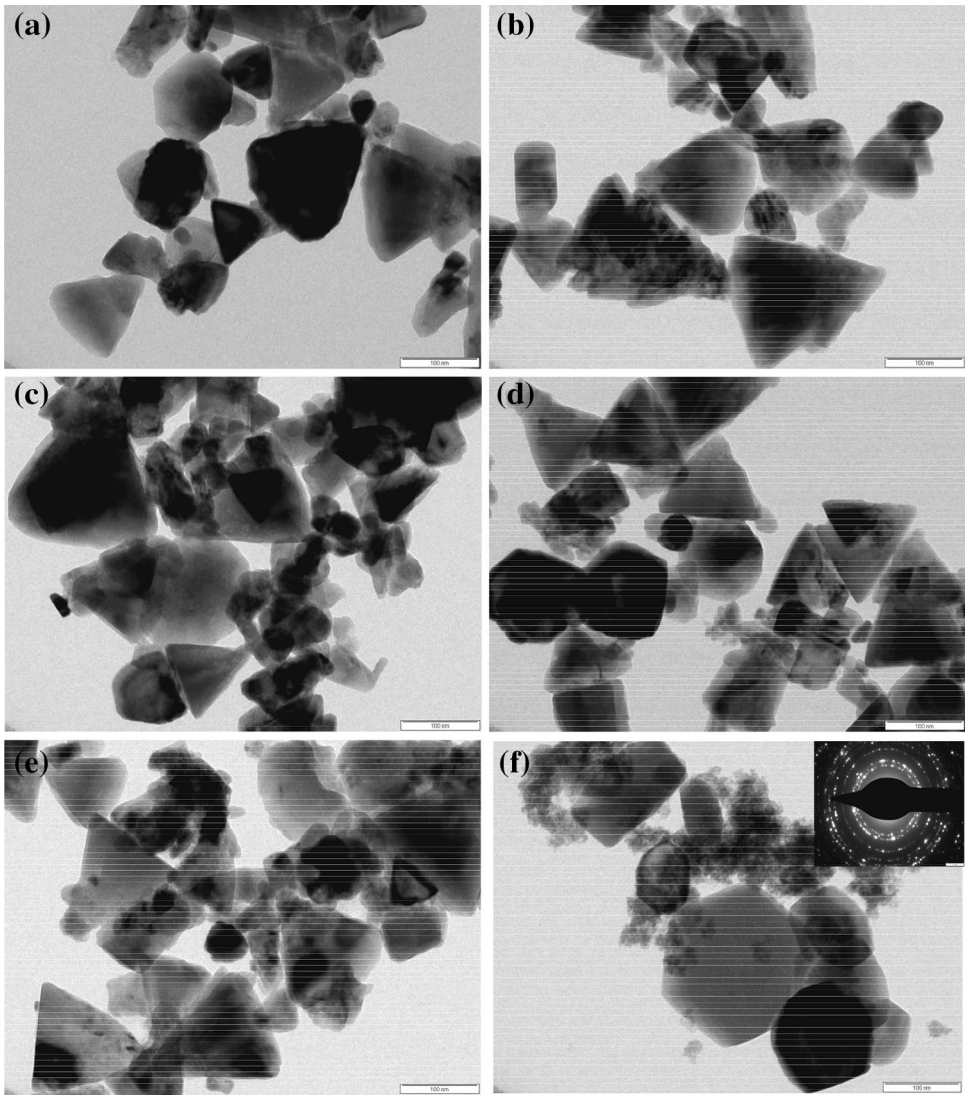

Fig. 8 TEM images of ZnO nanoparticles synthesized using chemical method; ZnO-S1 (**a**), and plant extracts; ZnO-S2 (**b**), ZnO-S3 (**c**), ZnO-S4 (**d**), ZnO-S5 (**e**), and ZnO-S6 (**f**) (*Inset* figure in (**f**): SAED pattern of ZnO-S6)

(ZnO-S5 and ZnO-S6, respectively) exhibited higher antioxidant activity than the other samples due to the presence of additional phytochemicals such as proteins and amino acids in these extracts along with carbohydrates, flavonoids, glycosides, phenolic compounds, saponins, and tannins.

Antidiabetic activity of ZnO nanoparticles

Diabetes mellitus results from defects in insulin secretion, insulin actions, or both, and is characterized by chronic hyperglycaemia with disturbed carbohydrate, fat, and protein metabolism. A strong inhibition of intestinal α-glucosidases and the mild inhibition of pancreatic α-amylase is an effective strategy for type II diabetes management [58]. Inhibitors used for the treatment of diabetes are α-amylase and α-glucosidase, which are the important enzymes in the carbohydrate metabolism. Delayed carbohydrate ingestion and glucose absorption with attenuation of post-prandial hyperglycaemic excursions is the result of inhibition of α-amylase and α-glucosidase. Therapeutic drugs such as acarbose, miglitol, and voglibose are currently used as α-glucosidase and α-amylase inhibitors [59]. The post-prandial lowering of blood glucose by α-glucosidase inhibitors such as acarbose and miglitol after a starch load is well established. The mechanism of action is through the inhibition of the last step in carbohydrate digestion, namely the conversion of disaccharide to monosaccharide (glucose) and a consequent decrease in the rate of entry of glucose into the systemic circulation [60]. The commercially available enzyme inhibitor such as acarbose is reported to have various side effects. Inhibitors from natural sources are of interest such as leaves of different plants due to their inhibitory potential against the target enzymes, which may be due to the presence of specific phenols [61].

In vitro α-amylase and α-glucosidase are useful, particularly when a large number of compounds are to be tested

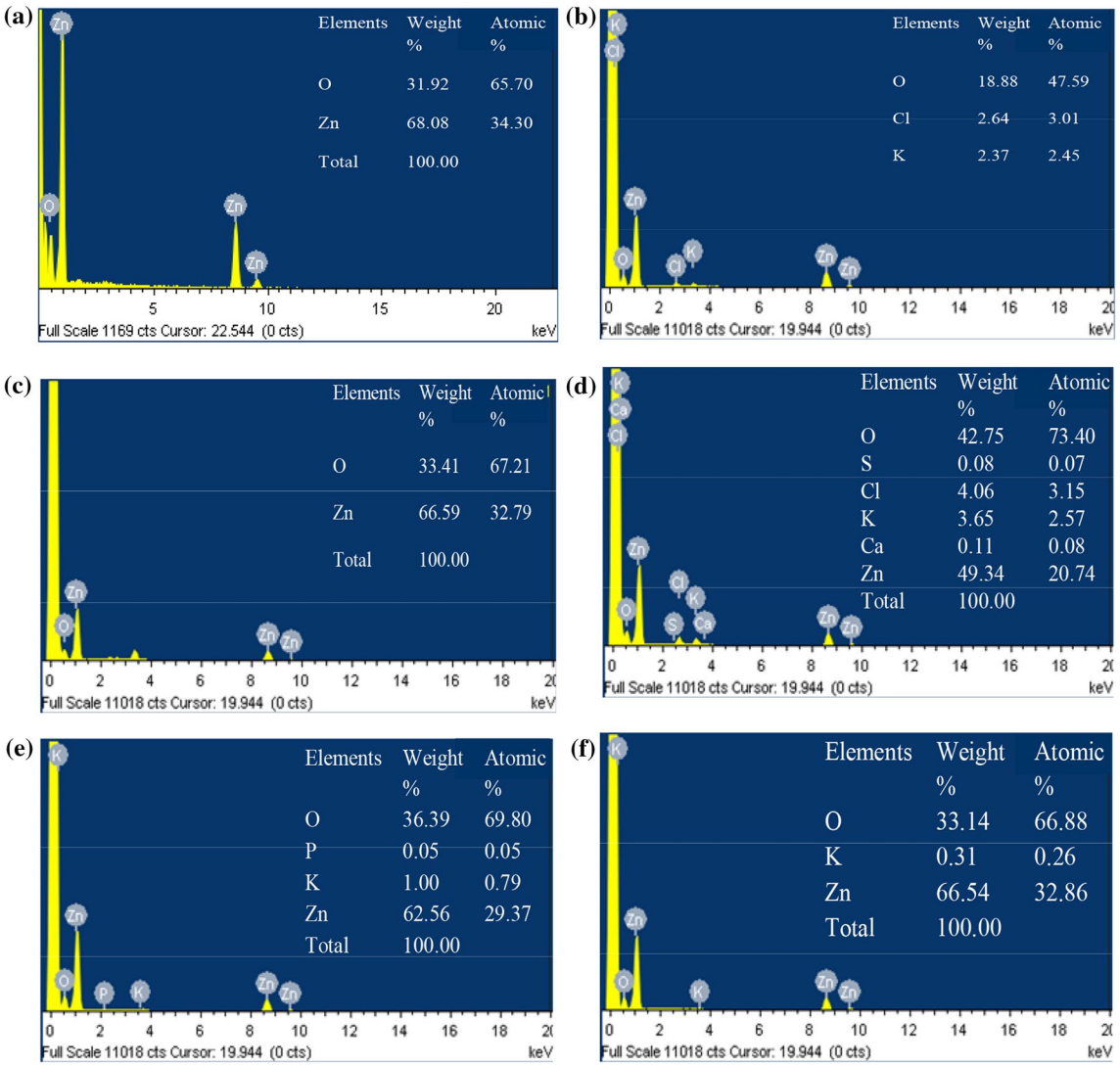

Fig. 9 EDX images of ZnO nanoparticles synthesized using chemical method; ZnO-S1 (**a**), and plant extracts; ZnO-S2 (**b**), ZnO-S3 (**c**), ZnO-S4 (**d**), ZnO-S5 (**e**), and ZnO-S6 (**f**)

Table 3 Antioxidant activity of ZnO nanoparticles tested by various methods

Samples	IC_{50} (μg/mL)*				
	ABTS assay	DPPH assay	Superoxide assay	H_2O_2 assay	*p*-NDA assay
ZnO-S1	>100	>100	>100	>100	>100
ZnO-S2	31.51 ± 0.200	37.8 ± 0.221	53.2 ± 0.211	58.4 ± 0.251	45.9 ± 0.31
ZnO-S3	25.53 ± 0.245	14.67 ± 0.244	31.6 ± 0.135	36.2 ± 0.2	26.28 ± 0.273
ZnO-S4	30.92 ± 0.303	36.46 ± 0.115	48.4 ± 0.342	54.6 ± 0.160	40.68 ± 0.117
ZnO-S5	11.47 ± 0.218	11.55 ± 0.100	24.4 ± 0.208	34.3 ± 0.229	23.54 ± 0.221
ZnO-S6	11.03 ± 0.302	11.49 ± 0.221	27.2 ± 0.230	31.4 ± 0.2	23.31 ± 0.335
Ascorbic acid	12.63 ± 0.195	7.65 ± 0.300	74.36 ± 0.176	78.6 ± 0.234	74.5 ± 0.170
Rutin	6.41 ± 0.196	8.16 ± 0.195	51.7 ± 0.251	36.6 ± 0.152	48.1 ± 0.334

*Average of three independent determinations

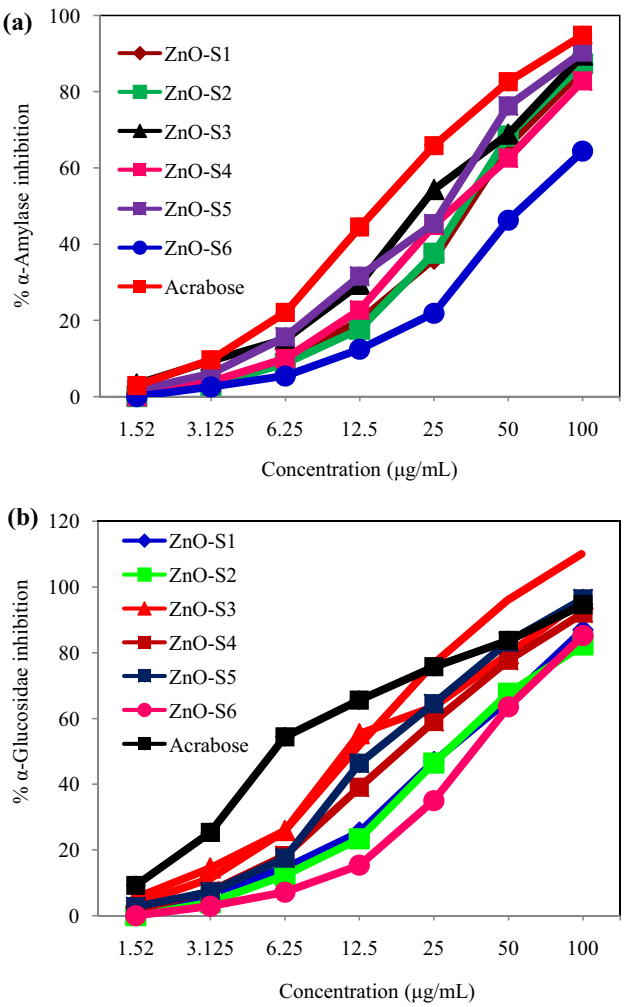

Fig. 10 Percentage α-amylase (**a**) and α-glucosidase (**b**) inhibition activity of ZnO nanoparticles synthesized using chemical and green methods

to rule out inactive compounds and save considerable time and money. The in vitro α-amylase inhibitory studies showed that the nanoparticles synthesized using *T. indica* (ZnO-S6) exhibited higher α-amylase inhibition activity when compared with ZnO nanoparticles synthesized using other plant extracts. The ZnO nanoparticles synthesized by chemical method exhibited the least antidiabetic activity. The % of inhibition showed a concentration-dependent reduction, which means that % of inhibition increased with increase in concentration (Fig. 10). The % of inhibition varied from 89 to 3.2% resulting an increase in % inhibition with increase in concentration.

In vitro α-glucosidase studies also revealed that ZnO nanoparticles synthesized using *T. indica* (ZnO-S6) exhibited higher α-glucosidase inhibition activity when compared with other ZnO nanoparticles. The highest concentration showed a maximum of 96% inhibition and the % of inhibition varied between 96 and 5.3% with respect to different concentration (Fig. 10). The in vitro studies of green synthesized ZnO nanoparticles exhibited appreciable α-amylase and α-glucosidase inhibitory activity causing delayed carbohydrate ingestion when compared with chemically synthesized ZnO nanoparticles (Tables 4, 5). From the obtained results, it can be concluded that the use of ZnO nanoparticles synthesized using the plant extracts will be greatly beneficial to reduce the rate of digestion and absorption of carbohydrate and thereby contribute for effective management of diabetes.

Conclusions

ZnO nanoparticles were synthesized using different plant extracts (*A. indica, H. rosa-sinensis, M. koenigi, M. oleifera*, and *T. indica*). For comparision purpose, the same ZnO nanoparticles was also synthesized by chemical method. The structure, morphology, and size of all the synthesized ZnO nanoparticles were examined by FT-IR, XRD, SEM, TEM, SAED, and EDX analysis. Preliminary phytochemicals analysis showed the presence of carbohydrates,

Table 4 Inhibitory effect of ZnO nanoparticles synthesized using chemical and green methods on α-amylase activity

Conc. (μg/mL)	% Inhibition						
	ZnO-S1	ZnO-S2	ZnO-S3	ZnO-S4	ZnO-S5	ZnO-S6	Acarbose
1.56	0.00 ± 0.00	0.00 ± 0.00	0.00 ± 0.00	0.00 ± 0.00	1.7 ± 0.86	3.27 ± 0.52	2.9 ± 0.25
3.125	2.53 ± 0.29	3.5 ± 0.56	3.87 ± 0.12	2.97 ± 0.35	6.07 ± 0.45	9.37 ± 0.44	9.63 ± 0.49
6.25	5.4 ± 0.31	8.87 ± 0.48	9.97 ± 0.29	8.73 ± 0.33	15.7 ± 0.81	15.03 ± 0.88	22.1 ± 0.65
12.5	12.4 ± 0.69	19.93 ± 1.41	22.73 ± 0.79	17.7 ± 0.44	31.6 ± 0.69	29.47 ± 0.87	44.47 ± 1.56
25	21.86 ± 1.16	36.1 ± 1.12	44.93 ± 0.97	37.6 ± 1.04	45.4 ± 0.81	54.33 ± 1.33	65.87 ± 1.54
50	46.3 ± 0.64	66 ± 1.22	62.53 ± 1.44	68.36 ± 2.11	76.27 ± 1.16	68.83 ± 1.26	82.64 ± 0.79
100	64.37 ± 0.56	85.7 ± 1.59	82.8 ± 0.95	87.33 ± 1.11	90.36 ± 1.11	89.56 ± 2.17	94.83 ± 0.95
IC_{50} (μg/mL)	97.68	60.41	38.93	59.9	35.72	28.63	16.25

Table 5 Inhibitory effect of ZnO nanoparticles synthesized using chemical and green methods on α-glucosidase activity

Conc. (μg/mL)	% Inhibition						
	ZnO-S1	ZnO-S2	ZnO-S3	ZnO-S4	ZnO-S5	ZnO-S6	Acarbose
1.56	0.00 ± 0.00	0.00 ± 0.00	1.83 ± 0.94	0.00 ± 0.00	2.73 ± 0.33	5.37 ± 0.38	9.2 ± 0.52
3.125	2.9 ± 0.32	6.63 ± 0.89	7.43 ± 0.59	3.93 ± 0.50	7.23 ± 0.55	14.43 ± 0.89	25.3 ± 1.65
6.25	7.13 ± 0.48	14.47 ± 1.16	18.3 ± 0.67	12.23 ± 0.91	17.47 ± 0.59	25.87 ± 0.91	54.4 ± 1.53
12.5	15.33 ± 0.38	25.37 ± 1.58	39.07 ± 1.45	23.4 ± 1.02	46.36 ± 1.11	55.33 ± 0.87	65.6 ± 1.51
25	34.97 ± 1.10	46.9 ± 0.69	59.07 ± 2.28	46.43 ± 1.36	64.53 ± 0.62	63.53 ± 1.31	75.73 ± 0.64
50	63.57 ± 1.24	65.56 ± 1.27	77.67 ± 1.74	67.7 ± 1.28	83.3 ± 0.91	79.6 ± 0.93	83.7 ± 1.49
100	85.2 ± 1.59	86.93 ± 0.84	92.03 ± 1.50	82.37 ± 2.16	96.37 ± 0.67	96.2 ± 1.34	94.63 ± 0.96
IC_{50} (μg/mL)	71.78	38.62	20.32	33.31	17.25	13.32	10.37

flavonoids, glycoside, phenolic compounds, proteins and amino acids, saponins, and tannins in the extracts. FT-IR spectra confirmed the presence of Zn–O bonding and XRD patterns revealed the hexagonal phase of ZnO. DRS-UV studies confirmed that ZnO nanoparticles had an average band-gap value of 3.19 eV. The results of antioxidant and antidiabetic activity show that the ZnO nanoparticles synthesized using the plant extracts of *M. oleifera* and *T. indica* (ZnO-S5 and ZnO-S6, respectively) exhibited higher activity due to the presence of proteins and amino acids along with other phytochemicals constituents. The obtained results are significant, but detailed mechanistic investigations are needed to establish better models for application in antidiabetic treatment.

Acknowledgements The authors are grateful to Sophisticated Analytical Instrumentation Facility, IIT B Mumbai 400 076, for providing TEM facility.

References

1. Sangeetha G, Rajeshwari S, Venckatesh R (2011) Green biosynthesis and characterization of zinc oxide nanoparticles using brown marine macroalga *Sargassum muticum* aqueous extract. Mat Res Bull 46:2560–2566
2. Premanathan M, Karthikeyan K, Jeyasubramanian K, Manivannan G (2011) Selective toxicity of ZnO nanoparticles toward Gram-positive bacteria and cancer cells by apoptosis through lipid peroxidation. Nanomed Nanotech Biol Med 7:184–192
3. Ramesh M, Anbuvannan M, Viruthagiri G (2014) Green synthesis of ZnO nanoparticles using *Solanum nigrum* leaf extract and their antibacterial activity. Spectrochim Acta A 136:864–870
4. Wu C, Qiao X, Chen J, Wang H, Tan F, Li S (2006) A novel chemical route to prepare ZnO nanoparticles. Mat Lett 60:1828–1832
5. Rajiv P, Rajeshwari S, Venckatesh R (2013) Bio-fabrication of zinc oxide nanoparticles using leaf extract of *Parthenium hysterophorus* L. and its size-dependent antifungal activity against plant fungal pathogens. Spectrochim Acta A 112:384–387
6. Anbuvannan M, Ramesh M, Viruthagiri G, Shanmugam N, Kannadasan N (2015) Synthesis, characterization and photocatalytic activity of ZnO nanoparticles prepared by biological method. Spectrochim Acta A 143:304–308
7. Gunalan S, Sivaraj R, Rajendran V (2012) Green synthesized ZnO nanoparticles against bacterial and fungal pathogens. Prog Nat Sci 22:693–700
8. Iravani S (2011) Green synthesis of metal nanoparticles using plants. Green Chem 13:2368–2650
9. Savoia D (2012) Plant-derived antimicrobial compounds: alternatives to antibiotics. Future Microbiol 7:979–990
10. Janaki AC, Sailatha E, Gunasekaran S (2015) Synthesis, characteristics and antimicrobial activity of ZnO nanoparticles. Spectrochim Acta A 144:17–22

11. Philip D (2010) Green synthesis of gold and silver nanoparticles using *Hibiscus rosa sinensis*. Physica E 42:1417–1424
12. Sangeetha G, Rajeshwari S, Venckatesh R (2011) Green synthesis of zinc oxide nanoparticles by *Aloe barbadensis* miller leaf extract: structure and optical properties. Mater Res Bull 46:2560–2566
13. Kuppusamy P, Yusoff MM, Parine NR, Govindan N (2015) Evaluation of in-vitro antioxidant and antibacterial properties of *Commelina nudiflora* L. extracts prepared by different polar solvents. Saudi J Biol Sci 22:293–301
14. Puri HS (1999) Plant sources, In: Hardman R (ed.) Neem. The divine tree. *Azadirachta indica*. Harwood Academic Publishers, Singapore
15. Adhirajan N, Kumar TR, Shanmugamsundaran N, Balu M (2003) In vivo and in vitro evaluation of hair growth potential of *Hibiscus rosa-sinensis* Linn. J Ethnopharmacol 88:235–239
16. Gilani AH, Bashir S, Janbaz KH, Shah AJ (2005) Presence of cholinergic and calcium channel blocking activities explains the traditional use of *Hibiscus rosa-sinensis* in constipation and diarrhoea. J Ethnopharmacol 102:289–294
17. Tachibana Y, Kikuzaki H, Lajis NH, Nakatani N (2001) Antioxidative activity of carbazoles from *Murraya koenigii* leaves. J Agric Food Chem 49:5589–5594
18. Mitra E, Ghosh AK, Ghosh D, Mukherjee D, Chattopadhyay A, Dutta S, Pattari SK, Bandhyopadhyay D (2012) Protective effect of aqueous curry leaf (*Murraya koenigii*) extract against cadmium-induced oxidative stress in rat heart. Food Chem Toxicol 50:1340–1353
19. Pruthi JS (1998) Spices and condiments, 5th edn. National Book Trust, India
20. Getie M, Gebre-Mariam T, Rietz R, Hohne C, Huschka C, Schmidtke M, Abate A, Neubert RHH (2003) Evaluation of the anti-microbial and anti-inflammatory activities of the medicinal plants *Dodonaea viscosa, Rumex nervosus* and *Rumex abyssinicus*. Fitoterapia 74:139–143
21. Barwala I, Sooda A, Sharma M, Singh B, Subhash C, Yadava (2013) Development of stevioside pluronic-F-68 copolymer based PLA-nanoparticles as an antidiabetic nanomedicine. Colloids Surf B 101:510–516
22. Khan BA, Abraham A, Leelamma S (1996) *Murraya koenigii* and *Brassica juncea*—alterations on lipid profile in 1–2 dimethyl hydrazine induced colon carcinogenesis. Invest New Drugs 14:365–369
23. Sreelatha S, Jeyachitra A, Padma PR (2011) Antiproliferation and induction of apoptosis by *Moringa oleifera* leaf extract on human cancer cells. Food Chem Toxicol 49:1270–1275
24. Singh RSG, Negi PS, Radha C (2013) Phenolic composition, antioxidant and antimicrobial activities of free and bound phenolic extracts of *Moringa oleifera* seed flour. J Funct Foods 5:1883–1891
25. Siddhuraju P (2007) Antioxidant activity of polyphenolic compounds extracted from defatted raw and dry heated *Tamarindus indica* seed coat. LWT-Food Sci Technol 40: 982–990
26. Maiti R, Jana D, Das UB, Ghosh D (2004) Antidiabetic effect of aqueous extract of seed of *Tamarindus indica* in streptozotocin-induced diabetic rats. J Ethnopharmacol 92:85–91
27. Bala N, Saha S, Chakraborty M, Maiti M, Das S, Basu R, Nandy P (2015) Green synthesis of zinc oxide nanoparticles using *Hibiscus subdariffa* leaf extract: effect of temperature on synthesis, anti-bacterial activity and anti-diabetic activity. RSC Adv 5:4993–5003
28. Murugadoss G (2012) ZnO/CdS nanocomposites: synthesis, structure and morphology. Particuology 10:722–728
29. Elumalai K, Velmurugan S, Ravi S, Kathiravan V, Ashokkumar S (2015) Bio-fabrication of zinc oxide nanoparticles using leaf extract of curry leaf (*Murraya koenigii*) and its antimicrobial activities. Mat Sci Semicon Process 34:365–372
30. Harborne JB (1973) Methods of plant analysis. In: Phytochemical methods. Chapman and Hall, London
31. Wagner H, Bladt S, Zgainski EM (1984) Plant drug analysis. Springer-Verlag, Berlin
32. Kokate CK (1994) Practical Pharmacognosy, 4th edn. Vallabh Prakashan, New Delhi
33. Re R, Pellegrini N, Proteggente A, Pannala A, Yang M, Rice EC (1999) Antioxidant activity applying an improved ABTS radical cation decolorization assay. Free Radic Biol Med 26:1231–1237
34. Inbathamizh L, Ponnu MT, Mary JE (2013) In vitro evaluation of antioxidant and anticancer potential of *Morinda pubescens* synthesized silver nanoparticles. J Pharm Res 6:32–38
35. Elizabeth K, Rao MNA (1990) Oxygen radical scavenging activity of curcumin. Int J Pharm 58:237–240
36. Jayaprakasha GK, Rao LJ, Sakariah KK (2004) Antioxidant activities of flavidin in different in vitro model systems. Bioorg Med Chem 12:5141–5146
37. Kim YM, Jeong YK, Wang MH, Lee WY, Rhee HI (2005) Inhibitory effect of pine extract on α-glucosidase activity and postprandial hyperglycemia. Nutrition 21:756–761
38. Sanap SP, Ghosh S, Jabgunde AM, Pinjari RV, Gejji SP, Singh S, Chopade BB, Dhavale DD (2010) Synthesis, computational study and glycosidase inhibitory activity of polyhydroxylated conidine alkaloids–a bicyclic iminosugar. Org Biomol Chem 8:3307–3315
39. Pan Y, He C, Wang H, Ji X, Wang K, Lui P (2010) Antioxidant activity of microwave-assisted extract of *Buddleia officinalis* and its major active component. Food chem 121:497–502
40. Elumalai K, Velmurugan S, Ravi S, Kathiravan V, Ashokkumar S (2015) Green synthesis of zinc oxide nanoparticles using *Moringa oleifera* leaf extract and evaluation of its antimicrobial activity. Spectrochim Acta A 143:158–164
41. Zak AK, Abrishami ME, Majid WHA, Yousefi R, Hosseini SM (2011) Effects of annealing temperature on some structural and optical properties of ZnO nanoparticles prepared by a modified sol–gel combustion method. Ceram Int 37:393–398
42. Nethravathi PC, Shruthi GS, Suresh D, Udaybhanu, Nagabhushana H, Sharma SC, (2015) *Garcinia xanthochymus* mediated green synthesis of ZnO nanoparticles: photoluminescence, photocatalytic and antioxidant activity studies. Ceram Int 41:8273–9202
43. Vanheusden K, Warren WL, Seager CH, Tallant DR, Voigt JA, Gnade BE (1996) Mechanisms behind green photoluminescence in ZnO phosphor powders. J Appl Phys 79:7983–7990
44. Shim ES, Kang HS, Pang SS, Kang JS, Yun I, Lee SY (2003) Annealing effect on the structural and optical properties of ZnO thin film on InP. Mater Sci Eng B 102:366–369
45. Bandyopadhyay S, Paul GK, Roy RR, Sen SK (2002) Study of structural and electrical properties of grain-boundary modified ZnO films prepared by sol–gel technique. Chem Phys 74:83–91
46. Jayaseelan C, Rahuman AA, Kirthi AV, Marimuthu S, Santhoshkumar T, Bagavan A, Gaurav K, Karthik L, Bhaskara Rao KV (2012) Novel microbial route to synthesize ZnO nanoparticles using *Aeromonas hydrophila* and their activity against pathogenic bacteria and fungi. Spectrochim Acta A 90:78–84
47. Ahmad N, Sharma Md S, Alam K, Singh VN, Shamsi SF, Mehta BR, Fatma A (2010) Rapid synthesis of silver nanoparticles using dried medicinal plant of basil. Colloids Surf B 81:81–86
48. Lewinski N, Colvin V, Drezek R (2008) Cytotoxicity of nanoparticles. Small 4:26–49

49. Gutteridge JMC, Rowley DA, Halliwell B (1981) Superoxide-dependent formation of hydroxyl radicals in the presence of iron salts. Biochem J 199:263–265
50. Nel A, Xia T, Madler L, Li N (2006) Toxic potential of materials at the nanolevel. Science 311:622–627
51. Sharma SK, Pujari PK, Sudarshan K, Dutta D, Mahapatra M, Godbole SV (2009) Positron annihilation studies in ZnO nanoparticles. Solid State Commun 149:550–554
52. Pal J, Chauhan P (2009) Structural and optical characterization of tin dioxide nanoparticles prepared by a surfactant mediated method. Mater Charact 60:1512–1516.
53. Cho K, Wang X, Nie S, Shin DM (2008) Therapeutic nanoparticles for drug delivery in cancer. Clin Cancer Res 14:1310–1316
54. Gulcin I, Kufrevioglu OI, Oktay M, Buyukokuroglu ME (2004) Antioxidant, antimicrobial, antiulcer and analgesic activities of nettle (*Urtica dioica* L.). J Ethnopharmacol 90:205–215
55. Ak T, Gulcin I (2008) Antioxidant and radical scavenging properties of curcumin. Chem Biol Interact 174:27–37
56. Halliwell B (1991) Reactive oxygen species in living systems: Source, biochemistry, and role in human disease. Am J Med 91:14–22
57. Nakayama T (1994) Suppression of hydroperoxide-induced cytotoxicity by polyphenols. Cancer Res 54:1991–1993
58. Krentz AJ, Baile CJ (2005) Oral antidiabetic agents. Drugs 65:385–411
59. Fred-Jaiyesimi A, Kio A, Richard W (2009) α-Amylase inhibitory effect of 3β-olean-12- en-3-yl (9Z)-hexadec-9-enoate isolated from *Spondias mombin* leaf. Food Chem 116:285–288
60. Joubert PH, Venter HL, Foukaridis GN (1990) The effect of miglitol and acarbose after an oral glucose load: a novel hypoglycaemic mechanism? Br J Clin Pharmacol 30:391–396
61. Sathya A, Siddhuraju P (2012) Role of phenolics as antioxidants, biomolecule protectors and as antidiabetic factors—evaluation on bark and empty pods of *Acacia auriculiformis*. Asian Pac J Trop 5:757–765